Joint Power Allocation for NOMA-Based Diamond Relay Networks With and Without Cooperation

BO-YING HUANG[1], YINMAN LEE [iD][2] (Member, IEEE), AND SOK-IAN SOU [iD][3] (Member, IEEE)

[1]Institute of Computer and Communication Engineering, National Cheng Kung University, Tainan 701, Taiwan

[2]Department of Electrical Engineering, National Chi Nan University, Puli 54561, Taiwan

[3]Department of Electrical Engineering, National Cheng Kung University, Tainan 701, Taiwan

CORRESPONDING AUTHOR: Y. LEE (e-mail: ymlee@ncnu.edu.tw)

ABSTRACT Non-orthogonal multiple access (NOMA)-based diamond relaying (NDR) is an efficient approach for combining NOMA and relaying techniques in such a way as to enhance the achievable rate from the source to the destination in the network. This paper examines the problem of joint power allocation among all the transmission phases during the operation of such networks. Based on the Karush-Kuhn-Tucker (KKT) condition and the second-order sufficient condition (SOSC), at least the local optimal solution is derived and analyzed. In addition, a new protocol for NDR networks based on cooperative communications is introduced and the associated joint power-allocation problem is examined. It is shown that this cooperative NDR (C-NDR) network further improves the achievable rate in some typical placements of the relays. Simulation results verify the correctness of the deviation and confirm the effectiveness of the proposed joint power-allocation method for both NDR and C-NDR networks.

INDEX TERMS Non-orthogonal multiple access (NOMA), relay networks, NOMA-based diamond relaying (NDR), cooperative communications, Karush-Kuhn-Tucker (KKT) condition, second-order sufficient condition (SOSC), joint power allocation, achievable rate.

I. INTRODUCTION

NON-ORTHOGONAL multiple access (NOMA) and relaying are both effective techniques for improving the performance of future wireless communication networks. NOMA allows multiple data streams to be transmitted simultaneously using the same resources, e.g., the same frequency bands or the same time slots, and is regarded as one of the most promising candidates for boosting the overall capacity of fifth-generation (5G) networks and beyond [1], [2]. NOMA technology can be applied in both the downlink direction and the uplink direction to achieve multiple access, and the success of most NOMA methods, e.g., power-domain NOMA, stems mainly from the difference in the locations of the transmitting/receiving devices accessing the network. For example, a device close to the access point (AP) and a second device far from the AP can both transmit/receive signals simultaneously [3]. In relay networks, one or more relays

are placed between the source and the destination to assist in forwarding the signals, thereby enhancing the wireless link reliability, increasing the system capacity, and/or extending the network coverage [4], [5]. Over the past decade, relaying technology has advanced tremendously both in sophistication and in scope, and many new modes of applicability have been proposed for wireless communications. For example, relays are now deployed extensively for cooperative communications, in which the AP and relays cooperate with one another to improve the communication quality, e.g., the capacity or diversity. Furthermore, relays are formally specified for use in cellular networks under Release 10 of the 4G Long-Term Evolution (LTE) standard [6], [7]. In addition, various relaying technologies have been proposed to facilitate the ultra-dense networks anticipated under 5G, including wireless backhaul for nomadic cells or data aggregation in the massive machine-type communications [8]–[11].

The literature contains many proposals for combining NOMA and relaying techniques to improve the network performance [12]–[35]. Many of these proposals are based on the concept of cooperative NOMA [12]–[14]. Specifically, the power-domain cooperative NOMA systems are first discussed in [12] and [13], in which the source sends superimposed data symbols to both the relay and the destination in the first phase. The relay is able to extract both symbols since it is close the source. However, the destination can obtain only the symbol with a larger power. Thus, in the second phase, the relay forwards the data symbols which the destination was unable to acquire in the first phase. In other words, the destination acquires two data symbols within two separate transmission phases. This is very different from conventional relay networks, in which the destination receives only a single data symbol over two transmission phases, and results in a significant improvement in the network throughput. The corresponding outage probability, diversity order, and capacity region are also examined in [12] and [13]. Later, the key features, opportunities, and challenges of this kind of cooperative NOMA networks are reviewed and summarized in [14]. The authors in [15]–[18] considered the relay selection problem in NOMA-based relay networks, while those in [19]–[22] examined the related power-allocation problem. In practice, both problems are of great importance since the relay location and power allocation both have a significant effect on the NOMA/relaying behavior, and thus also impact the overall performance of the network. To be more specific, in [15], a two-stage relay-selection approach is proposed to achieve a better outage probability than some related schemes, including the well-known max-min relay-selection method. In [16], another two-stage method is examined focusing on various relaying protocols with different quality-of-service (QoS) requirements, and more analytical results are provided. More sophisticated relay-selection approaches with adaptive power allocation according to changing environments are proposed in [17] and [18]. The authors in [19] consider a new way for selecting an optimal relay mode and optimal transmission power levels simultaneously in NOMA-based relay networks to achieve a better network throughput. Furthermore, the spectral efficiency of amplify-and-forward (AF)-based NOMA cooperation is investigated in [20], while a similar problem is tackled for decode-and-forward (DF)-based NOMA cooperation as well in [22]. The problem of joint resource allocation, involving the subcarrier pair, subcarrier-user assignment, and power levels, is examined to maximize the network throughput in [21]. Typically, it is formulated as a mixed-integer nonlinear programming problem, which is then solved via a special divide-and-conquer strategy. Besides, the effect of employing different relaying protocols, including the classical AF, DF, and various hybrid approaches with or without direct link, to the power-allocation method, network throughput, diversity order, outage probability, and even energy efficiency is explored in [23]–[26]. In general, the results show that the application of different relaying protocols

according to different circumstances is highly beneficial for enhancing the robustness of the relaying operation. The authors in [27]–[29] combined the full-duplex (FD) mode with NOMA relaying to further improve the performance. The gain from FD is shown, and the timing for switching between half-duplex (HD) and FD is also discussed. Last but not least, the authors in [30]–[33] combine a new energy-harvesting (EH) technique with the concept of simultaneous wireless information and power transfer (SWIPT) to reduce the total energy consumption of the network. The focus is how EH/SWIPT can benefit the network in terms of different performance measures. Different factors such as the number of relays used, the protocol chosen, and the power splitting strategy are included in the discussion for prolonging the lifetime of the energy-constrained relay network.

NOMA-based diamond relaying, in which a pair of relays perform signal reception similar to downlink NOMA and signal transmission similar to uplink NOMA, respectively, provides an effective approach for improving the achievable rate from the source to the destination compared to most traditional two-relay protocols [34], [35], which will be explained more in the next section. In this study, the achievable rate of this NOMA-based diamond relaying is further enhanced through jointly allocating the power assigned to the downlink and uplink NOMA operations, respectively. The main contributions of this study can be summarized as follows:

1) The joint power allocation problem is described as an optimization problem, in which successive-interference cancellation (SIC) constraints are explicitly imposed in order to ensure the success of both downlink NOMA and uplink NOMA during actual implementation. In consequence, all power levels in the NOMA operation are jointly optimized, and this generally leads to a better achievable rate.

2) The Karush-Kuhn-Tucker (KKT) condition [36] for the joint power-allocation problem is derived, and the solution is obtained and checked with the second-order sufficient condition (SOSC). This means at least a local optimum is reached. In addition, new insights are provided into the settings of the NDR network. It is shown that the proposed power-allocation method results in a higher achievable rate than other related methods for the considered dual-hop NDR network; particularly in the case where the two relays are placed rather asymmetrically, i.e., one relay is close to the source while the other is close to the destination. The effect of this asymmetric relay placement on the power allocation (and hence the overall achievable rate) is analyzed and discussed.

3) The concept of cooperative communications is applied to the NDR network. The KKT condition for the resultant cooperative NDR (C-NDR) network is derived and the related joint power-allocation problem is examined as well. It is shown that the C-NDR network with
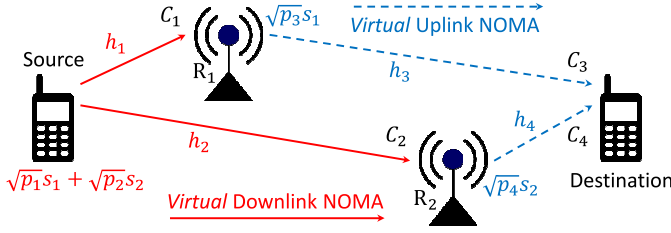
FIGURE 1. Network model of the NDR scheme where the source intends to send superimposed data symbols to the destination with two NOMA-functioned relays.

the proposed joint power allocation further improves the achievable rate of NDR in some typical relay-placement scenarios, e.g., both NOMA-functioned relays are closer to the destination than to the source. Design guidelines about how to place the two relays and allocate the power jointly are additionally provided for both the NDR network and the C-NDR network.

The remainder of this paper is organized as follows. Section II provides the related background to the present research and derives both the network model of the NDR and the related achievable rate. Section III presents the joint power-allocation problem for NDR and derives the solution. Section IV introduces the proposed C-NDR network and examines the associated joint power-allocation problem for improving the achievable rate further. Section V presents and discusses the simulation results for the performance of the proposed joint power-allocation methods for NDR and C-NDR, respectively. Finally, Section VI provides some brief concluding remarks.

II. NETWORK MODEL OF NOMA-BASED DIAMOND RELAYING (NDR)

This section commences by introducing the network model of the conventional NDR scheme. A mathematical expression for the achievable rate of the network is then derived.

The study considers the two-relay network shown in Fig. 1 consisting of a source, two relays (R_1 and R_2), and a destination. An assumption is made that each member of the network has a single-antenna and half-duplex capability. Furthermore, "downlink NOMA" and "uplink NOMA" concepts are both *virtually* employed to enhance the achievable rate from the source to the destination.[1] As shown in Fig. 1, R_1 is placed close to the source and far from the destination, while R_2 is placed far from the source but close to the destination. Such a relaying scenario was first proposed in [34], [35], and is referred to as a NOMA-based diamond relay (NDR) network. It was shown in [34], [35] that by employing the idea of NOMA virtually for signal reception/transmission at the two relays, the achievable rate of the network can be significantly improved compared to conventional two-relay networks, as explained in the following.

1. The word *virtual* or *virtually* is taken to mean here that only the idea of NOMA is used for signal transmission and reception. In other words, it is not the usual usage of NOMA, in which different users transmit or receive their corresponding signals simultaneously using the same radio resources.

Also shown in Fig. 1, the channels of the four included transmission paths are denoted by h_1, h_2, h_3 and h_4, respectively; moreover, we let $g_1 = |h_1|^2$, $g_2 = |h_2|^2$, $g_3 = |h_3|^2$ and $g_4 = |h_4|^2$ for notational simplicity. Two transmission phases are required for the source to send data symbols to the destination through the use of the two NOMA-functioned relays. In the first phase, the source transmits the superimposed data symbols $\sqrt{P_1}s_1 + \sqrt{P_2}s_2$ to both relays with P_1 and P_2 denoting the power levels for s_1 and s_2, respectively. It is not difficult to see that this resembles a downlink-NOMA scenario. According to the conventional downlink NOMA operation, to ensure the decoding of this downlink NOMA-like transmission is performed adequately, it is appropriate to set $P_1 < P_2$ since the distance between the source and R_1 is shorter than that between the source and R_2, in which $g_1 > g_2$ is expected. Both relays then receive the signal sent by the source. At R_1, s_2 is first decoded due to the larger value of P_2. Assume that s_2 can be correctly decoded. SIC is then performed in which s_2 is subtracted from the received signal of R_1. This results in a clean version of the received signal for s_1, and s_1 is decoded at R_1 afterward. At the same time, at R_2, s_2 is decoded directly also thanks to its better signal quality, and s_1 is treated as background noise. Therefore, R_1 obtains s_1 while R_2 obtains s_2, and the first phase of NDR is completed. During the second phase, R_1 forwards s_1 with P_3 to the destination and R_2 forwards s_2 with P_4 to the destination simultaneously. Likewise, $g_3 < g_4$ is expected due to the differences in the distances of R_1 to the destination and R_2 to the destination. Again, with suitable values of P_3 and P_4, we see that this resembles an uplink-NOMA scenario. That is, upon receiving the two superimposed signals at the destination, the possibly stronger component s_2 from R_2 is decoded first. SIC is then performed to subtract s_2 from the received signal. Finally, s_1 is extracted as well from the resultant signal. As a consequence, both s_1 and s_2 can be recovered at the destination. Usually, in order to guarantee the success of the SIC operation in both downlink NOMA and uplink NOMA, the signal-to-noise ratio (SNR) of the stronger signal must be greater than that of the weaker one up to a certain value. Here, we set such SIC constraints necessary for the considered NDR network as

$$\frac{P_2 g_1/N_0}{P_1 g_1/N_0} \geq \gamma_{\text{th}} \tag{1}$$

$$\frac{P_4 g_4/N_0}{P_3 g_3/N_0} \geq \gamma_{\text{th}} \tag{2}$$

where N_0 denotes the noise power level, and γ_{th} is a preset threshold value. With the success of SIC in both virtual downlink NOMA and uplink NOMA, the achievable rate (in bits per second per Hertz, bps/Hz) for the four transmission paths, also indicated in Fig. 1, can be calculated to be

$$C_1 = \log_2\left(1 + \frac{P_1 g_1}{N_0}\right), \quad \text{for } s_1 \text{ at } R_1 \tag{3}$$

$$C_2 = \log_2\left(1 + \frac{P_2 g_2}{P_1 g_2 + N_0}\right), \quad \text{for } s_2 \text{ at } R_2 \qquad (4)$$

$$C_3 = \log_2\left(1 + \frac{P_3 g_3}{N_0}\right), \quad \text{for } s_1 \text{ at Dest.} \qquad (5)$$

$$C_4 = \log_2\left(1 + \frac{P_4 g_4}{P_3 g_3 + N_0}\right), \quad \text{for } s_2 \text{ at Dest.} \qquad (6)$$

Note that in fact the destination obtains s_1 from R_1 and s_2 from R_2, respectively. The overall achievable rate at the destination is the sum of C_3 for s_1 and C_4 for s_2. Therefore, the achievable rate at the destination can be expressed as

$$y = \frac{1}{2}(C_3 + C_4) \qquad (7)$$

where the factor $\frac{1}{2}$ is involved due to the use of two transmission phases. In general, with suitable settings of power levels and relay locations in the NDR network, a better achievable rate can be obtained by virtue of the reception of two information streams.

III. PROPOSED JOINT POWER ALLOCATION FOR NDR

Here, we examine the problem of maximizing the overall achievable rate at the destination through jointly selecting the four power levels P_1, P_2, P_3 and P_4. As stated in the previous section, two information symbols are obtained at the destination simultaneously in the NDR network, and the corresponding achievable rate is depicted in (7). Intuitively, both C_3 and C_4 are required to be maximized. However, letting C_3 and C_4 increase without bound only may be irrational. To see this, we imagine that the upper branch and the lower branch in Fig. 1 are analogous to two pipes in which water flows from the frond-end to the back-end. It is not possible that the amount of water in the back-end is larger than that in the frond end. Back to the NDR scenario, in consequence, both $C_3 > C_1$ and $C_4 > C_2$ cannot happen. To describe the inflow of information must be larger than the outflow of information at both relays, accordingly, we need to add the following two conditions

$$C_1 \geq C_3 \qquad (8)$$

$$C_2 \geq C_4. \qquad (9)$$

In addition, the sum of all power values P_1, P_2, P_3 and P_4 should be limited by an allowable total transmit power value, i.e., $P_1 + P_2 + P_3 + P_4 \leq P_t$ is required. Collecting all these constraints, we can formulate an optimization problem to maximize the overall achievable rate at the destination with respect to the four power levels as

$$\max_{P_1,P_2,P_3,P_4} \quad \frac{1}{2}(C_3 + C_4)$$
$$\text{subject to} \quad C_1 \geq C_3$$
$$C_2 \geq C_4$$
$$\frac{P_2 g_1 / N_0}{P_1 g_1 / N_0} \geq \gamma_{th}$$
$$\frac{P_4 g_4 / N_0}{P_3 g_3 / N_0} \geq \gamma_{th}$$

$$P_1 + P_2 + P_3 + P_4 \leq P_t$$
$$P_i \geq 0, \quad i = 1, 2, 3, 4. \qquad (10)$$

To deal with the problem in (10), the objective function y to be maximized is first rewritten as

$$y = \frac{1}{2}(C_3 + C_4)$$
$$= \frac{1}{2}\left[\log_2\left(1 + \frac{P_3 g_3}{N_0}\right) + \log_2\left(1 + \frac{P_4 g_4}{P_3 g_3 + N_0}\right)\right] \qquad (11)$$
$$= \frac{1}{2\ln 2}\left[\ln\left(1 + \frac{P_3 g_3}{N_0}\right) + \ln\left(1 + \frac{P_4 g_4}{P_3 g_3 + N_0}\right)\right]. \qquad (12)$$

We see that $\frac{1}{2\ln 2}$ in (12) is merely a scalar that does not affect the result of the optimization, and the expression in (12) is much easier to be differentiated than that in (11) due to the use of the natural logarithmic function. Here, we let $-[\ln(1 + \frac{P_3 g_3}{N_0}) + \ln(1 + \frac{P_4 g_4}{P_3 g_3 + N_0})]$ be our new objective function to be minimized instead of the original one. For the sake of simplicity, $C_1 \geq C_3$ and $C_2 \geq C_4$ are expressed as

$$P_1 g_1 - P_3 g_3 \geq 0 \qquad (13)$$

$$P_2 g_2 (P_3 g_3 + N_0) - P_4 g_4 (P_1 g_2 + N_0) \geq 0. \qquad (14)$$

Also, the two SIC constraints in (10) can be simplified to become

$$P_2 - \gamma_{th} P_1 \geq 0 \qquad (15)$$

$$P_4 g_4 - \gamma_{th} P_3 g_3 \geq 0. \qquad (16)$$

As a result, the optimization problem in (10) can be restated to be

$$\min_{P_1,P_2,P_3,P_4} \quad -\left[\ln\left(1 + \frac{P_3 g_3}{N_0}\right) + \ln\left(1 + \frac{P_4 g_4}{P_3 g_3 + N_0}\right)\right]$$
$$\text{subject to} \quad -(P_1 g_1 - P_3 g_3) \leq 0$$
$$- \left[P_2 g_2 (P_3 g_3 + N_0) - P_4 g_4 (P_1 g_2 + N_0)\right] \leq 0$$
$$- (P_2 - \gamma_{th} P_1) \leq 0$$
$$- (P_4 g_4 - \gamma_{th} P_3 g_3) \leq 0$$
$$- (P_t - P_1 - P_2 - P_3 - P_4) \leq 0$$
$$- P_i \leq 0, \quad i = 1, 2, 3, 4 \qquad (17)$$

which is in the standard form. Apparently, (17) is a constrained minimization problem. Due to the inclusion of the flow constraint in (14), the problem does not pass the convexity test, which is described in Appendix A, and thus (17) is not a convex optimization problem [37]. Here, we tackle it directly using Karush-Kuhn-Tucker (KKT) Theorem [36]. The critical points found are then checked with the SOSC to determine whether they are strict local minimizers. To be more specific, first of all, the Lagrangian function L can be set to be

$$L = -\ln\left(1 + \frac{P_3 g_3}{N_0}\right) - \ln\left(1 + \frac{P_4 g_4}{P_3 g_3 + N_0}\right)$$
$$- \lambda_1 (P_1 g_1 - P_3 g_3)$$
$$- \lambda_2 \left[P_2 g_2 (P_3 g_3 + N_0) - P_4 g_4 (P_1 g_2 + N_0)\right]$$

$$- \lambda_3(P_2 - \gamma_{\text{th}}P_1)$$
$$- \lambda_4(P_4g_4 - \gamma_{\text{th}}P_3g_3)$$
$$- \lambda_5(P_t - P_1 - P_2 - P_3 - P_4)$$
$$- \lambda_6P_1 - \lambda_7P_2 - \lambda_8P_3 - \lambda_9P_4 \tag{18}$$

where λ_i ($i = 1, 2, \ldots, 9$) are the KKT multipliers. After some calculation, the necessary conditions for the solution from KKT theorem can be shown to consist of the following equalities and inequalities:

$$\lambda_i \geq 0, \quad i = 1, 2, \ldots, 9 \tag{19}$$

$$\frac{\partial L}{\partial P_1} = g_1\lambda_1 - P_4g_2g_4\lambda_2 - \gamma_{\text{th}}\lambda_3 - \lambda_5 + \lambda_6 = 0 \tag{20}$$

$$\frac{\partial L}{\partial P_2} = g_2(P_3g_3 + N_0)\lambda_2 + \lambda_3 - \lambda_5 + \lambda_7 = 0 \tag{21}$$

$$\frac{\partial L}{\partial P_3} = -g_3\lambda_1 + P_2g_2g_3\lambda_2 - \gamma_{\text{th}}g_3\lambda_4 - \lambda_5 + \lambda_8$$
$$+ \frac{g_3}{P_3g_3 + N_0}$$
$$- \frac{P_4g_3g_4}{(P_4g_4 + P_3g_3 + N_0)(P_3g_3 + N_0)} = 0 \tag{22}$$

$$\frac{\partial L}{\partial P_4} = -g_4(P_1g_2 + N_0)\lambda_2 + g_4\lambda_4 - \lambda_5 + \lambda_9$$
$$+ \frac{g_4}{P_4g_4 + P_3g_3 + N_0} = 0 \tag{23}$$

$$\lambda_1(P_1g_1 - P_3g_3) = 0 \tag{24}$$

$$\lambda_2[P_2g_2(P_3g_3 + N_0) - P_4g_4(P_1g_2 + N_0)] = 0 \tag{25}$$

$$\lambda_3(P_2 - \gamma_{\text{th}}P_1) = 0 \tag{26}$$

$$\lambda_4(P_4g_4 - \gamma_{\text{th}}P_3g_3) = 0 \tag{27}$$

$$\lambda_5(P_t - P_1 - P_2 - P_3 - P_4) = 0 \tag{28}$$

$$\lambda_6P_1 = 0 \tag{29}$$

$$\lambda_7P_2 = 0 \tag{30}$$

$$\lambda_8P_3 = 0 \tag{31}$$

$$\lambda_9P_4 = 0 \tag{32}$$

$$P_1g_1 - P_3g_3 \geq 0 \tag{33}$$

$$P_2g_2(P_3g_3 + N_0) - P_4g_4(P_1g_2 + N_0) \geq 0 \tag{34}$$

$$P_2 - \gamma_{\text{th}}P_1 \geq 0 \tag{35}$$

$$P_4g_4 - \gamma_{\text{th}}P_3g_3 \geq 0 \tag{36}$$

$$P_t - P_1 - P_2 - P_3 - P_4 \geq 0 \tag{37}$$

$$P_i \geq 0, \quad i = 1, 2, 3, 4. \tag{38}$$

In order to find a solution satisfying the conditions from (19) to (38), we need to examine the feasibility of all these conditions. Appendix B gives the detailed discussions, and we find that some variables can be ignored to largely simplify the calculation of finding the critical points. For example, we have $\lambda_6 = \lambda_7 = \lambda_8 = \lambda_9 = 0$. Also, for λ_3 and λ_4, there are only two possibilities: $\lambda_3 = \lambda_4 = 0$ or $\lambda_3 = 0$ with $\lambda_4 > 0$. In consequence, the number of equalities is enough for finding the solution of all variables and the inequalities can be used for checking the feasibility of the solution. Thanks to the derivations and the related simplification, the
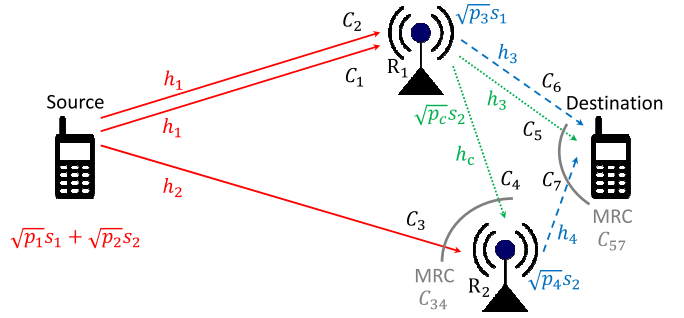

FIGURE 2. Network model of cooperative NOMA-based diamond relay (C-NDR) network where the source sends overlapped pieces of information to the destination.

complexity of locating the critical points numerically can be almost negligible.

After finding the critical points, the SOSC is used to check if they are the strict local minimizers we expect. Since the Lagrangian function L given in (18) contains quite many variables, the calculation of the general Hessian may be quite complicated, and is too tedious to express in closed form. As an alternative, we check it dynamically during simulations. Details are given in the simulation section.

In Section V, simulation results are provided to show the performance of the considered NDR network with this joint power allocation.

IV. COOPERATIVE NOMA-BASED DIAMOND RELAYING (C-NDR)

This section proposes a new cooperative protocol for NDR networks, referred to as cooperative NDR (C-NDR). The optimal joint power-allocation problem for the C-NDR network is derived and an investigation is then performed to examine the effectiveness of the C-NDR approach in improving the overall achievable rate from the source to the destination compared to that in a conventional NDR network.

A. NETWORK MODEL AND ACHIEVABLE RATE OF C-NDR

As in the conventional NDR network, the source in the C-NDR network also attempts to transmit two sets of data information to the destination through two NOMA-functioned relays (R_1 and R_2). However, in the C-NDR case, three transmission phases are employed rather than two, as shown in Fig. 2. In the first phase, the mixed data information $\sqrt{P_1}s_1 + \sqrt{P_2}s_2$ is sent over channels h_1 and h_2 to relays R_1 and R_2, respectively. (Note that an assumption is made that $g_1 > g_2$ such that $P_1 < P_2$ and virtual downlink NOMA can be adequately performed.) The data symbol s_1 at R_1 is obtained via SIC, in which s_2 is decoded first and is then subtracted from the received signal before decoding s_1. Meanwhile, R_2 decodes s_2 directly treating s_1 as noise due to the setting $P_2 > P_1$. Since h_2 is relatively weak in the network, the quality of s_2 at R_2 may be inadequate for the next transmission phase. However, R_1 already owns data

symbol s_2 from the prior SIC operation, and therefore forwards it to both R_2 and the destination in order to enhance the quality of s_2 intentionally. In other words, C-NDR incorporates an additional cooperation phase, in which R_1 sends s_2 to both R_2 over channel h_c and the destination over channel h_3 with a transmit power level P_c in both cases. At R_2, maximal ratio combining (MRC) is used to combine the s_2 data symbols received in the first phase and cooperation phase, respectively, for better quality. At the destination, the additional pieces of the data symbol s_2 will also be utilized later. In the third phase, R_1 and R_2 send s_1 and s_2 to the destination simultaneously with powers P_3 and P_4, respectively, in accordance with the uplink NOMA concept. Given suitable settings of P_3 and P_4, and exploiting the fact that P_3, SIC is performed at the destination; with s_2 being decoded first and then subtracted from the received signal prior to decoding s_1. As described above, a copy of s_2 is also received at the destination in the preceding cooperation phase. Consequently, MRC is also employed to further enhance the quality of s_2 at the destination and decode s_1 more smoothly as a result. This completes the new protocol for C-NDR.

As mentioned, Fig. 2 is the network model of the considered C-NDR. Although the model is quite similar to that of NDR in Fig. 1, some additional notations are needed. For example, h_c is used to denote the channel between R_1 and R_2, and $g_c = |h_c|^2$. Also, P_c is the power used in the cooperation phase. In the following, we investigate the joint power-allocation problem of C-NDR. Again, the constraints for the success of the two SIC operations during the first and the third phases are represented as

$$\frac{P_2 g_1 / N_0}{P_1 g_1 / N_0} \geq \gamma_{\text{th}} \tag{39}$$

$$\frac{P_4 g_4 / N_0}{P_3 g_3 / N_0} \geq \gamma_{\text{th}}. \tag{40}$$

For this C-NDR scheme in the first phase, R_1 decodes both s_2 and s_1 by virtue of the SIC, and so we may write the achievable rate C_1 for s_2 and C_2 for s_1, respectively, at R_1. At the same time, R_2 decodes s_2 directly to obtain the rate C_3. Thus, we have

$$C_1 = \log_2\left(1 + \frac{P_2 g_1}{P_1 g_1 + N_0}\right), \quad \text{for } s_2 \text{ at } R_1 \tag{41}$$

$$C_2 = \log_2\left(1 + \frac{P_1 g_1}{N_0}\right), \quad \text{for } s_1 \text{ at } R_1 \tag{42}$$

$$C_3 = \log_2\left(1 + \frac{P_2 g_2}{P_1 g_2 + N_0}\right), \quad \text{for } s_2 \text{ at } R_2. \tag{43}$$

To enhance the quality of s_2, R_1 forwards s_2 to R_2 and the destination in the cooperation phase. If we only count this part of s_2 at R_2 during this phase, the achievable rate can be written as

$$C_4 = \log_2\left(1 + \frac{P_c g_c}{N_0}\right), \quad \text{for } s_2 \text{ at } R_2. \tag{44}$$

Note that R_2 actually owns two independent sets of s_2. We let R_2 conduct MRC to restore s_2 from both phases, and then we obtain the improved achievable rate as

$$C_{34} = \log_2\left(1 + \left(\frac{P_2 g_2}{P_1 g_2 + N_0} + \frac{P_c g_c}{N_0}\right)\right),$$
$$\text{for } s_2 \text{ at } R_2 \text{ after MRC.} \tag{45}$$

On the other hand, the destination receives s_2 from R_1 in the cooperation phase, and this standalone achievable rate can be expressed as

$$C_5 = \log_2\left(1 + \frac{P_c g_3}{N_0}\right), \quad \text{for } s_2 \text{ at Dest.} \tag{46}$$

Finally, in the third phase, R_1 transmits s_1 and R_2 transmits s_2 to the destination at the same time. By virtue of the virtual uplink NOMA, the rate C_6 for s_1 at the destination and C_7 for s_2 at the destination can be written as

$$C_6 = \log_2\left(1 + \frac{P_3 g_3}{N_0}\right), \quad \text{for } s_1 \text{ at Dest.} \tag{47}$$

$$C_7 = \log_2\left(1 + \frac{P_4 g_4}{P_3 g_3 + N_0}\right), \quad \text{for } s_2 \text{ at Dest.} \tag{48}$$

respectively. Unlike the conventional NDR, the destination actually receives two sets of s_2 within different phases thanks to the cooperation. We may apply MRC again to combine those for s_2, and the overall achievable rate at the destination can then be presented as

$$y_c = \frac{1}{3}(C_6 + C_{57}) \tag{49}$$

with

$$C_{57} = \log_2\left(1 + \left(\frac{P_c g_3}{N_0} + \frac{P_4 g_4}{P_3 g_3 + N_0}\right)\right),$$
$$\text{for } s_2 \text{ at Destination after MRC} \tag{50}$$

and the factor $\frac{1}{3}$ in (49) is due to the use of three transmission phases.

B. JOINT POWER ALLOCATION FOR C-NDR

Similarly, we try to jointly tune the power levels P_1, P_2, P_c, P_3 and P_4 to maximize the overall achievable rate of the C-NDR network given in (49). In order to fulfill this task, we formulate a new optimization problem. Since the expressions for the achievable rate of this new protocol are more complicated than those without the cooperation phase, we need to rearrange the conditions for the problem first. Based on the concept of network flows mentioned before, the following four constraints must be set, i.e.,

$$C_1 \geq C_4, \quad \text{for } s_2 \text{ in } h_1-\text{path and } h_c-\text{path} \tag{51}$$

$$C_1 \geq C_5, \quad \text{for } s_2 \text{ in } h_1-\text{path and } h_3-\text{path} \tag{52}$$

$$C_2 \geq C_6, \quad \text{for } s_1 \text{ in } h_1-\text{path and } h_3-\text{path} \tag{53}$$

$$C_{34} \geq C_7, \quad \text{for } s_2 \text{ in } h_2-\text{path}+h_c-\text{path}$$
$$\text{and } h_4-\text{path} \tag{54}$$

Also, the sum of all power levels is limited by the total power P_t used, namely,

$$P_1 + P_2 + P_3 + P_4 + P_c \leq P_t \qquad (55)$$

and the SIC constraints given in (39) and (40) are still adequate for this case. Then, we arrange these conditions and formulate the optimization as

$$\max_{P_1, P_2, P_3, P_4, P_c} \frac{1}{3}(C_6 + C_{57})$$

$$\text{subject to} \quad C_1 \geq C_4$$
$$C_1 \geq C_5$$
$$C_2 \geq C_6$$
$$C_{34} \geq C_7$$
$$\frac{P_2 g_1 / N_0}{P_1 g_1 / N_0} \geq \gamma_{th}$$
$$\frac{P_4 g_4 / N_0}{P_3 g_3 / N_0} \geq \gamma_{th}$$
$$P_1 + P_2 + P_3 + P_4 + P_c \leq P_t$$
$$P_i \geq 0, \quad i = 1, 2, 3, 4, c. \qquad (56)$$

To solve this problem, again, we transform the objective function into another one with natural logarithmic functions only, and perform the necessary simplification. The problem in (56) is then equivalently changed to

$$\min_{P_1, P_2, P_3, P_4, P_c} \quad -\left[\ln\left(1 + \frac{P_3 g_3}{N_0}\right)\right.$$
$$\left. + \ln\left(1 + \frac{P_4 g_4}{P_3 g_3 + N_0} + \frac{P_c g_3}{N_0}\right)\right]$$

$$\text{subject to} \quad -\left[N_0 P_2 g_1 - P_c g_c(P_1 g_1 + N_0)\right] \leq 0$$
$$-\left[N_0 P_2 g_1 - P_c g_3(P_1 g_1 + N_0)\right] \leq 0$$
$$-\left[P_1 g_1 - P_3 g_3\right] \leq 0$$
$$-\{N_0 P_2 g_2(P_3 g_3 + N_0)$$
$$+ (P_1 g_2 + N_0)\left[P_c g_c(P_3 g_3 + N_0)\right.$$
$$\left. - N_0 P_4 g_4\right]\} \leq 0$$
$$-(P_2 - \gamma_{th} P_1) \leq 0$$
$$-(P_4 g_4 - \gamma_{th} P_3 g_3) \leq 0$$
$$-(P_t - P_1 - P_2 - P_3 - P_4 - P_c) \leq 0$$
$$-P_i \leq 0, \quad i = 1, 2, 3, 4, c. \qquad (57)$$

Likewise, we employ the same approach as that in Appendix A to check if (57) is a convex optimization problem. It can be found that the flow constraint in (54) is not a convex function. This essentially lets the optimization problem posed in (57) not convex. With the use of the Lagrange multipliers μ_i $(i = 1, 2, \ldots, 12)$, the Lagrangian function L_c of it is written as

$$L_c = -\ln\left(1 + \frac{P_3 g_3}{N_0}\right) - \ln\left(1 + \frac{P_4 g_4}{P_3 g_3 + N_0} + \frac{P_c g_3}{N_0}\right)$$
$$- \mu_1\left[N_0 P_2 g_1 - P_c g_c(P_1 g_1 + N_0)\right]$$
$$- \mu_2\left[N_0 P_2 g_1 - P_c g_3(P_1 g_1 + N_0)\right]$$
$$- \mu_3(P_1 g_1 - P_3 g_3)$$

$$- \mu_4\{N_0 P_2 g_2(P_3 g_3 + N_0)$$
$$- (P_1 g_2 + N_0)[P_c g_c(P_3 g_3 + N_0) - N_0 P_4 g_4]\}$$
$$- \mu_5(P_2 - \gamma_{th} P_1)$$
$$- \mu_6(P_4 g_4 - \gamma_{th} P_3 g_3)$$
$$- \mu_7(P_t - P_1 - P_2 - P_3 - P_4 - P_c)$$
$$- \mu_8 P_1 - \mu_9 P_2 - \mu_{10} P_3 - \mu_{11} P_4 - \mu_{12} P_c. \qquad (58)$$

Hence, the necessary conditions by KKT theorem can be listed as

$$\mu_i \geq 0, \quad i = 1, 2, \ldots, 12 \qquad (59)$$

$$\frac{\partial L_c}{\partial P_1} = -g_1 g_c P_c \mu_1 - g_1 g_3 P_c \mu_2 + g_1 \mu_3$$
$$+ \left[g_2 g_c P_c(P_3 g_3 + N_0) - N_0 g_2 g_4 P_4\right]\mu_4$$
$$- \gamma_{th} \mu_5 - \mu_7 + \mu_8 = 0 \qquad (60)$$

$$\frac{\partial L_c}{\partial P_2} = N_0 g_1 \mu_1 + N_0 g_1 \mu_2 + N_0 g_2(P_3 g_3 + N_0)\mu_4$$
$$+ \mu_5 - \mu_7 + \mu_9 = 0 \qquad (61)$$

$$\frac{\partial L_c}{\partial P_3} = \frac{g_3}{P_3 g_3 + N_0}$$
$$- \frac{g_3 g_4 P_4}{\left(1 + \frac{P_4 g_4}{P_3 g_3 + N_0} + \frac{P_c g_3}{N_0}\right)(P_3 g_3 + N_0)^2}$$
$$- g_3 \mu_3 + \left[g_3 g_c P_c(P_1 g_2 + N_0) + N_0 P_2 g_2 g_3\right]\mu_4$$
$$- \gamma_{th} g_3 \mu_6 - \mu_7 + \mu_{10} = 0 \qquad (62)$$

$$\frac{\partial L_c}{\partial P_4} = \frac{g_4}{\left(1 + \frac{P_4 g_4}{P_3 g_3 + N_0} + \frac{P_c g_3}{N_0}\right)(P_3 g_3 + N_0)}$$
$$- N_0 g_4(P_1 g_2 + N_0)\mu_4 + g_4 \mu_6 - \mu_7 + \mu_{11} = 0 \qquad (63)$$

$$\frac{\partial L_c}{\partial P_c} = \frac{g_3}{N_0\left(1 + \frac{P_4 g_4}{P_3 g_3 + N_0} + \frac{P_c g_3}{N_0}\right)} - g_c(P_1 g_1 + N0)\mu_1$$
$$- g_3(P_1 g_1 + N_0)\mu_2$$
$$+ g_4(P_1 g_2 + N_0)(P_3 g_3 + N_0)\mu_4$$
$$- \mu_7 + \mu_{12} = 0 \qquad (64)$$

$$\mu_1\left[N_0 P_2 g_1 - P_c g_c(P_1 g_1 + N_0)\right] = 0 \qquad (65)$$
$$\mu_2\left[N_0 P_2 g_1 - P_c g_3(P_1 g_1 + N_0)\right] = 0 \qquad (66)$$
$$\mu_3(P_1 g_1 - P_3 g_3) = 0 \qquad (67)$$
$$\mu_4\{N_0 P_2 g_2(P_3 g_3 + N_0)$$
$$+ (P_1 g_2 + N_0)\left[P_c g_c(P_3 g_3 + N_0) - N_0 P_4 g_4\right]\} = 0 \quad (68)$$
$$\mu_5(P_2 - \gamma_{th} P_1) = 0 \qquad (69)$$
$$\mu_6(P_4 g_4 - \gamma_{th} P_3 g_3) = 0 \qquad (70)$$
$$\mu_7(P_t - P_1 - P_2 - P_3 - P_4 - P_c) = 0 \qquad (71)$$
$$\mu_8 P_1 = 0 \qquad (72)$$
$$\mu_9 P_2 = 0 \qquad (73)$$
$$\mu_{10} P_3 = 0 \qquad (74)$$
$$\mu_{11} P_4 = 0 \qquad (75)$$
$$\mu_{12} P_c = 0 \qquad (76)$$

$$P_1 g_1 - P_3 g_3 \geq 0 \qquad (77)$$

$$P_2 g_2 (P_3 g_3 + N_0) - P_4 g_4 (P_1 g_2 + N_0) \geq 0 \qquad (78)$$

$$P_2 - \gamma_{\text{th}} P_1 \geq 0 \qquad (79)$$

$$P_4 g_4 - \gamma_{\text{th}} P_3 g_3 \geq 0 \qquad (80)$$

$$P_t - P_1 - P_2 - P_3 - P_4 - P_c \geq 0 \qquad (81)$$

$$P_i \geq 0, \quad i = 1, \ 2, \ 3, \ 4, \ c. \qquad (82)$$

These necessary conditions are simplified and discussed in depth in Appendix C. As a result, the critical points can be instantly found as well. Similar to the approach for NDR, we employ the SOSC to check whether the solution is the strict local optimum we look for.

In the next section, simulations are also used to reveal the performance of the C-NDR network with the proposed joint power allocation, and, importantly, under what situations this C-NDR network will further benefit the overall achievable rate from the source to the destination.

V. SIMULATION RESULTS

This section conducts simulations to verify the correctness of the derivations presented above and to confirm the effectiveness of the proposed joint power-allocation methods for the NDR and C-NDR networks. In the present study, the performance of the proposed joint power-allocation method is first compared to that of the three approaches considered in [35], namely "I-CSI": a power-allocation method based on instantaneous channel state information (CSI); "S-CSI": a power-allocation method based on statistical CSI; and "sub. S-CSI": a suboptimal power-allocation method based on S-CSI. We also include the three conventional protocols for two-relay networks, i.e., the MRC, Max-Min, and distributed beamforming (DBF), for comparison. The detailed operations of these three protocols can be found in [35].

A. NDR

The simulations commence by examining the achievable rate of NDR under the proposed joint power-allocation method given different relay placements to see the performance of our power-allocation scheme and how the relay locations affect the performance. As mentioned in Sections III and IV-B, KKT theorem is first used to find the critical points for the power levels, and the SOSC is then employed to check whether they are the strict local minimizers. Based on some typical parameter values (a special case chosen from the following settings), Appendix D demonstrates how we make use of the SOSC to examine the solution found by the KKT condition.

In the first set of simulations, the channels are modelled as independently distributed complex-Gaussian random variables with zero mean and the variances shown in Table 1. In addition, a scaling factor M is used to vary the channel variances in order to reflect changes in the locations of the two relays relative to the source and destination. For example, a larger value of M is applied to indicate an increasing distance of the two relays from the source and hence a closer distance

TABLE 1. Parameters used in simulations for Fig. 3.

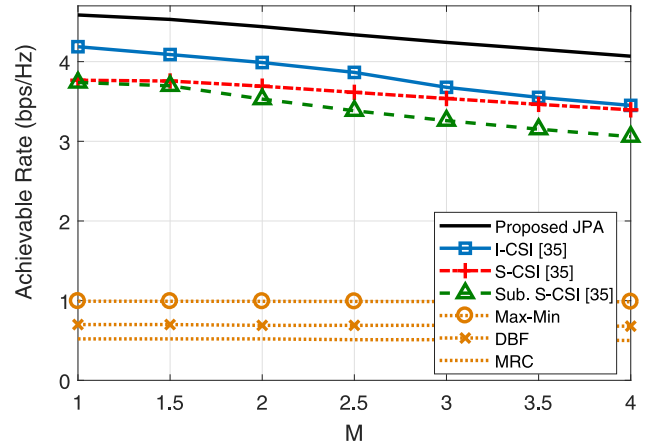| Parameter	Quantity
Variance of channel h_1 (σ_1^2)	$10/M$
Variance of channel h_2 (σ_2^2)	$3/M$
Variance of channel h_3 (σ_3^2)	$5M$
Variance of channel h_3 (σ_4^2)	$9M$
Decoding threshold for the SIC (γ_{th})	5
Total transmit power (P_t)	2
Noise power (N_0)	10^{-2}
Scaling factor for the variance of channels (M)	1 to 4

FIGURE 3. Overall achievable rate vs. M for various approaches experiencing random channels set according to Table 1.
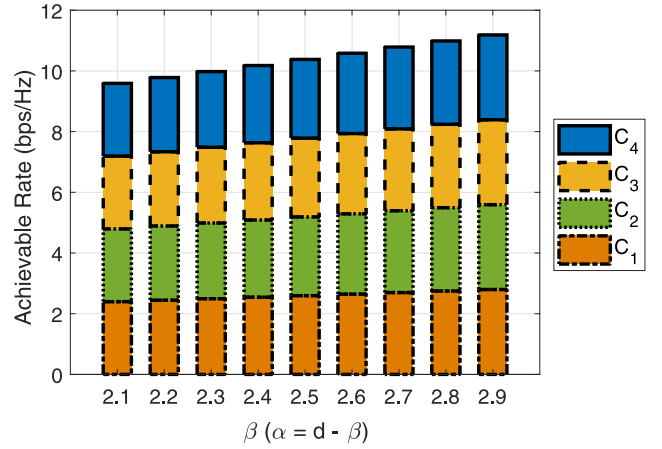
to the destination. Fig. 3 shows the overall achievable rate of the NDR network under the four power-allocation methods for different values of M. (Note that the label "JPA" indicates the joint power-allocation method proposed in the present study.) As shown, the JPA method results in a higher achievable rate than any of the methods proposed in [35] and the three conventional protocols for all values of M. For the proposed JPA and the three power-allocation methods in [35], the achievable rate reduces with increasing M since, as M increases, the channels in the first phase become weaker, and this inevitably imposes a performance bottleneck on the second phase. However, due to the flow balance concept incorporated within JPA, a greater amount of power is used in the first phase, which sustains the achievable rate in the second phase and equalizes the performance over the two transmission phases as a result. Consequently, irrespective of the value of M, the achievable rate of NDR under JPA is greater than that under any of the other schemes in [35]. Besides, as M increases, the achievable rate of all three conventional protocols does not change much and is quite behind from that of JPA. Because the MRC protocol requires more time slots to accomplish the whole transmission from the source to the destination than both Max-Min and DBF, it is the worst among the three conventional protocols in terms of the achievable-rate performance. In general, the results confirm the practical performance advantage of allocating the power resources jointly between the two transmission phases, as proposed in the present study.

TABLE 2. Parameters used in simulations for Fig. 5, Fig. 6, and Fig. 7.

Parameter	Quantity
Distance between the source and R_1 (α)	$d - \beta$
Distance between the source and R_2 (β)	2.1 to 2.9
Distance between the source and the destination (d)	4
Path loss exponent (n)	2
Decoding threshold for the SIC (γ_{th})	5
Total transmit power (P_t)	2
Noise power (N_0)	10^{-2}
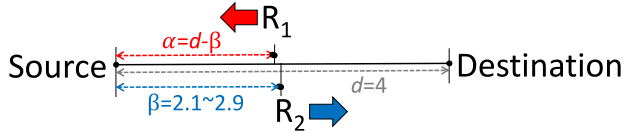
FIGURE 4. Plan of relay placement for Table 2, Fig. 5, Fig. 6, and Fig. 7.
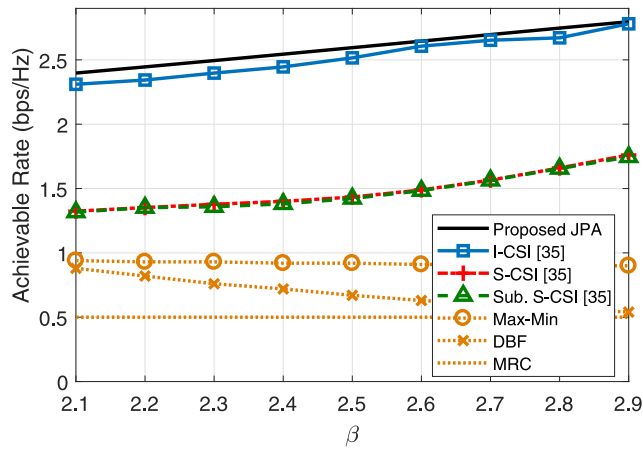
FIGURE 5. Overall achievable rate vs. β for various approaches experiencing path-loss only channels set according to Table 2.

FIGURE 6. Achievable rate of the four transmission paths for NDR with joint power allocation given in Fig. 5.
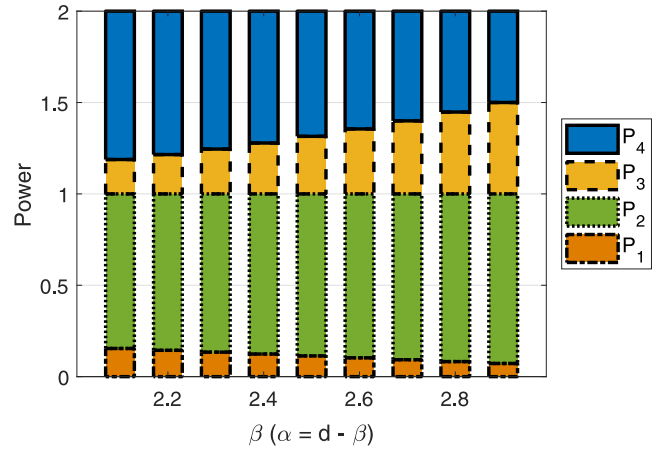
FIGURE 7. Power levels in the four transmission paths for NDR with joint power allocation given in Fig. 5.

Second, we discuss the performance of NDR with JPA and other methods in another scenario. To investigate the effect of the relay placement on the NDR achievable rate more thoroughly, a further series of simulations is performed using a path-loss only channel model with the parameter settings shown in Table 2. Note that in Table 2, it is assumed that the source, the two relays (R_1, R_2) and the destination all lie on a straight line, as shown in Fig. 4. The distance between the source and the destination is denoted as d, while the distance between the source and R_1 is denoted as α. Similarly, the distance between the source and R_2 is denoted as β. In assigning the parameter values used in the simulations, the condition $\alpha < \beta < d = 4$ is imposed. Referring to Fig. 4, as the value of β increases, the distance between the two relays increases and α decreases. In other words, R_1 moves toward the source and R_2 moves toward the destination. That is, both relays move further from the midpoint position between the source and destination. Fig. 5 shows that for all values of β, the achievable rate of NDR under the proposed JPA scheme is higher than that under any of the power-allocation methods in [35]. Generally speaking, for the proposed JPA and the three

power-allocation methods in [35], as the two relays move further away from the midpoint between the source and the destination, the achievable rate improves since, under this situation, the NOMA condition is more thoroughly accomplished. Besides, as β increases, the achievable-rate performance of both Max-Min and MRC does not vary much as well while that of DBF degrades gradually due to the enlarged distance between the two relays. Fig. 6 shows the achievable rate of each path in the NDR network under the proposed JPA method for various placements of the relays. The results show that the flow balance concept is basically maintained among the four paths in the two transmission phases, irrespective of the placement of the two relays. Fig. 7 shows the corresponding power levels (P_1, P_2, P_3 and P_4) in the four paths. It is seen that as β increases, P_3 increases and P_4 decreases commensurately. This power arrangement maintains the flow balance in the upper and lower branches of the NDR, and hence enables virtual uplink-NOMA in the second phase to perform more smoothly. As a result, the overall achievable rate is improved.

TABLE 3. Parameters used in simulations for Fig. 9, Fig. 10, and Fig. 11.

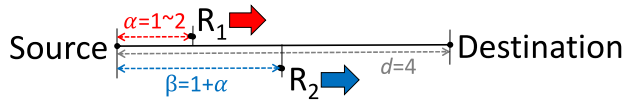| Parameter	Quantity
Distance between the source and R_1 (α)	1 to 2
Distance between the source and R_2 (β)	$1 + \alpha$
Distance between the source and the destination (d)	4
Path loss exponent (n)	2
Decoding threshold for the SIC (γ_{th})	5
Total transmit power (P_t)	2
Noise power (N_0)	10^{-2}

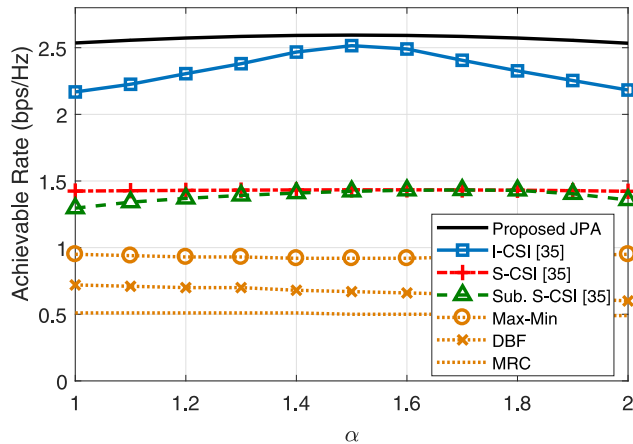**FIGURE 8.** Plan of relay placement for Table 3, Fig. 9, Fig. 10, and Fig. 11.

FIGURE 9. Overall achievable rate vs. α for various approaches experiencing path-loss only channels set according to Table 3.

FIGURE 10. Achievable rate of the four transmission paths for NDR with joint power allocation given in Fig. 9.
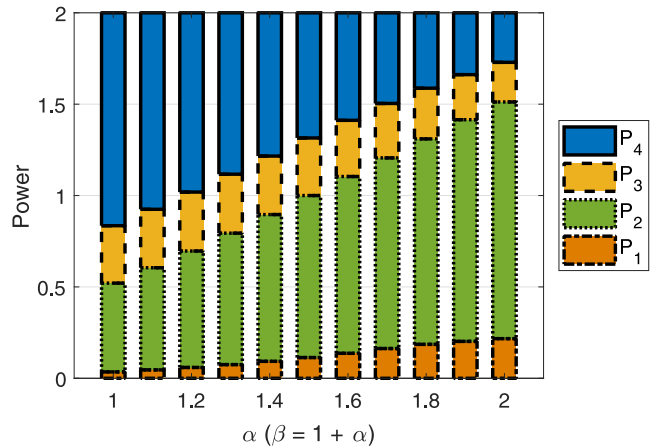
FIGURE 11. Power levels in the four transmission paths for NDR with joint power allocation given in Fig. 9.

Further simulations are performed using the same path-loss only channel model shown in Fig. 8, but with the parameters shown in Table 3. In this circumstance, as α increases, both relays moves from near the source to near the destination. The corresponding simulation results are presented in Figs. 9 to 11. The results in Fig. 9 confirm that the JPA method consistently achieves the highest achievable rate among all the considered methods. It is noted that, for the proposed JPA and the three power-allocation methods in [35], the achievable rate first increases and then decreases with increasing α. In other words, the achievable rate performance of all four schemes improves as the two relays approach the midpoint position between the source and the destination. For all values of α, the three conventional protocols still perform much worse than those with power allocation. Observing Fig. 10, it is seen that the proposed JPA method maintains an approximately constant achievable rate in each path irrespective of the placement of the two relays. Again, the flow-balance concept is valid. Furthermore, Fig. 11 shows that P_1 and P_2 increase, while P_3 and P_4 decrease, as the two relays move further from the source. This result is reasonable since as the relays move away from the source and toward the destination, the channel conditions in the first transmission phase change from good
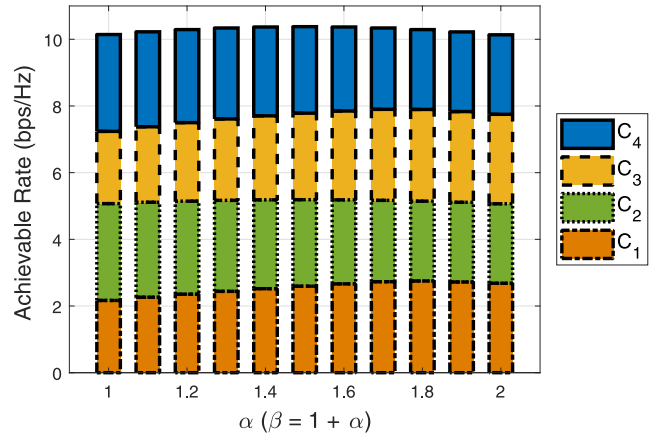
to bad, while those in the second phase change from bad to good. In other words, the power levels in the first phase need to be increased, while those in the second phase need to be decreased, to maintain a balance between the flows.

B. C-NDR

Having investigated the performance of the proposed JPA method for the conventional NDR network, further simulations are conducted to evaluate the achievable rate of JPA in the proposed C-NDR network.

The simulations commence by considering the random-channel model with the parameter settings given in Table 4. As shown, the scaling factor M is again used to simulate the movement of the relays away from the source and toward the destination. Typically, the variance of g_c equals that of g_3. However, since the channels are randomly generated in the present case, g_c may not necessarily be the same as g_3 every time. The optimal power levels for the considered model are obtained using the derivations given in Section IV-B. Fig. 12 compares the achievable rates of C-NDR and NDR under their corresponding JPA methods. When M is small, i.e., both

TABLE 4. Parameters used in simulations for Fig. 12.

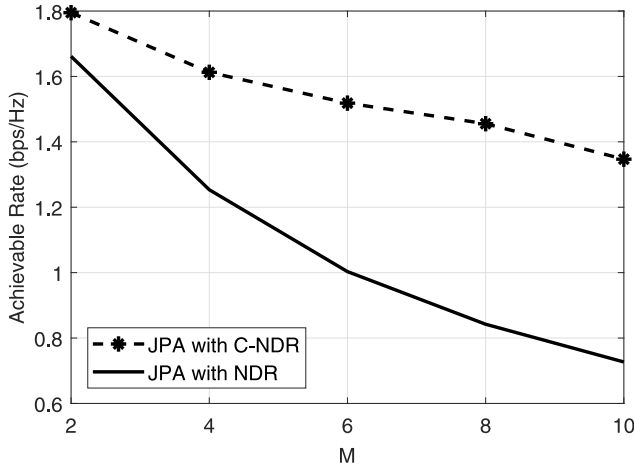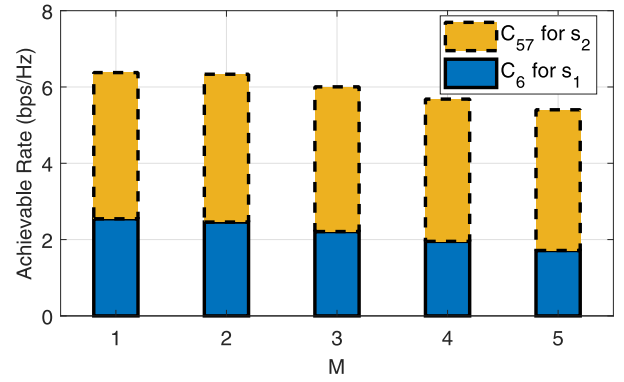| Parameter	Quantity
Variance of channel h_1 (σ_1^2)	$5/M$
Variance of channel h_2 (σ_2^2)	$1/M$
Variance of channel h_3 (σ_3^2)	$2M$
Variance of channel h_4 (σ_4^2)	$6M$
Variance of channel h_c (σ_c^2)	$2M$
Threshold for successful SIC (γ_{th})	5
Total transmit power (P_t)	2
Noise power (N_0)	10^{-1}
Scaling factor for channel variance (M)	2 to 10

FIGURE 12. Overall achievable rate vs. *M* for NDR and C-NDR with joint power allocation under random channels.

TABLE 5. Parameters used in simulations for Fig. 12, Fig. 13, Fig. 14, Fig. 15, Fig. 16, and Fig. 17.

Parameter	Quantity
Variance of channel h_1	$5/M$
Variance of channel h_2	$1/M$
Variance of channel h_3	$2M$
Variance of channel h_4	$6M$
Variance of channel h_c	$2.1M$
Decoding threshold for the SIC (γ_{th})	5
Total transmit power (P_t)	2
Noise power (N_0)	10^{-1}
Scaling factor for the variance of channels (M)	1 to 5

FIGURE 13. Achievable rate of C_6 for s_1 and C_{57} for s_2 vs. *M* for C-NDR with joint power allocation under the settings of Table 4.
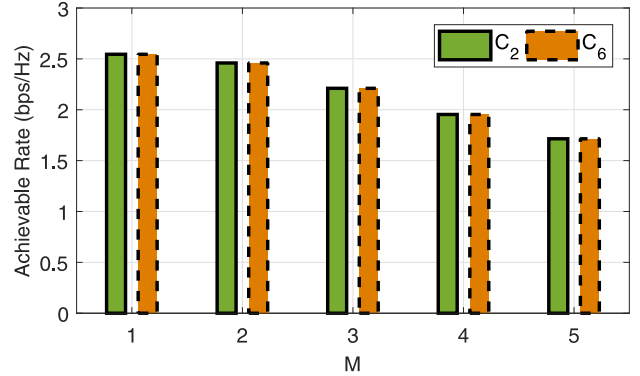
FIGURE 14. Achievable rate of C_2 and C_6 vs. *M* for C-NDR with joint power allocation under the settings of Table 4.
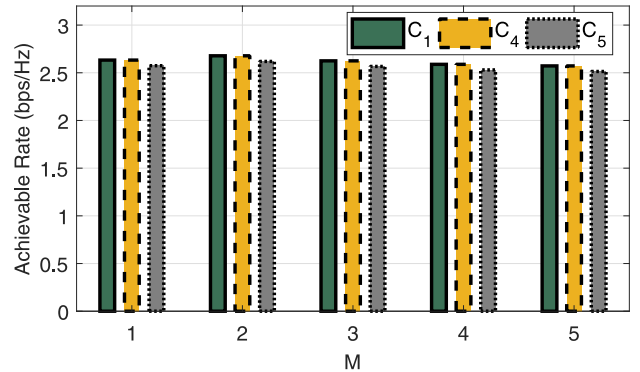
FIGURE 15. Achievable rate of C_1, C_4 and C_5 vs. *M* for C-NDR with joint power allocation under the settings of Table 4.

relays are close to the source, the two networks have a similar achievable rate. As *M* increases, i.e., the relays move toward the destination, the achievable rate reduces in both networks due to the corresponding reduction in the channel quality in both paths during the first phase. However, the achievable rate of C-NDR is significantly higher than that of NDR since the C-NDR scheme enhances the quality of s_2 at both R_2 and the destination. Hence, the result in Fig. 12 depicts that the additional cooperation phase in C-NDR can remedy the degradation of achievable rate quite effectively in the scenario that both relays are much close to the destination.

A final series of simulations is performed using the parameter settings shown in Table 5 to further investigate the effect of C-NDR under the proposed JPA method on the achievable rate. As shown, the variance of h_c is set slightly larger than that of h_3 in order to simulate the case where the distance

between the two relays is shorter than that between R_2 and the destination. Figs. 13 to 17 show the corresponding results for the achievable rate and power levels given different values of the scaling factor, *M*. Referring to Fig. 13, it is seen that the achievable rates of s_1 and s_2 at the destination are maintained at an acceptable level even when *M* is large. The results presented in Figs. 14 to 16 confirm that JPA maintains a flow balance within the network as the relays move toward the destination, i.e., $C_2 \approx C_6$ in Fig. 14, $C_1 \approx C_4 \approx C_5$ in Fig. 15, and $C_{34} \approx C_7$ in Fig. 16. Finally, Fig. 17 shows
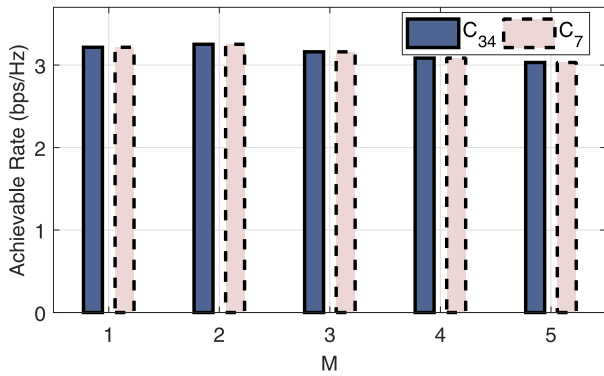
FIGURE 16. Achievable rate of C_{34} and C_7 vs. M for C-NDR with joint power allocation under the settings of Table 4.
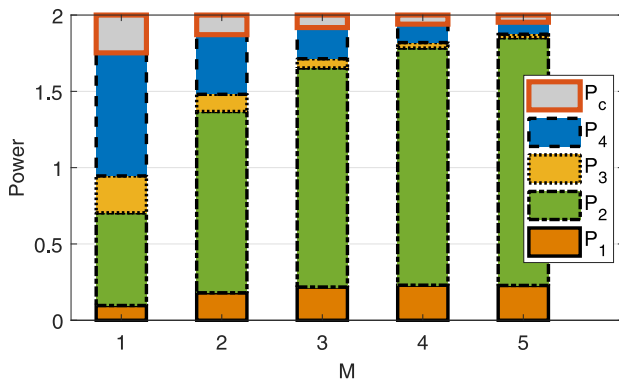

FIGURE 17. Power levels in the four transmission paths for C-NDR with joint power allocation under the settings of Table 4.

that P_1 and P_2 increase, while P_3, P_4 and P_c decrease, as M increases. In other words, as the relays move toward the destination, P_1 and P_2 are increased in order to provide an improved basis for the achievable rate in the latter phases. However, with a reduced distance between the relays and the destination, the channel conditions in the second (cooperation) and third phases improve, and consequently lower values of P_3, P_4 and P_c are sufficient to preserve a similar achievable-rate performance.

VI. CONCLUSION

Relaying and NOMA are both proven techniques for enhancing the network capacity. This paper has proposed a method for improving the achievable rate of NDR networks by means of a joint power-allocation approach. At least the local optimum of the resultant problem has been derived and examined. A new protocol, designated as C-NDR, has been proposed in which an additional cooperation phase is added to the conventional NDR communication protocol. The related joint power-allocation problem has also been addressed. The simulation results have shown that the proposed joint power-allocation methods result in a higher achievable rate in the NDR and C-NDR networks than that obtained using other state-of-the-art approaches. The effects of the relay placement on the achievable-rate performance

have been examined. In general, the results provide useful design guidelines for improving the performance of relay-based NOMA networks in real-world implementations.

APPENDIX A

A convex optimization problem is an optimization problem in which the objective function is a convex function and the feasible set is a convex set. As mentioned, the flow constraint in (14) is not convex, which makes the problem in (17) not a convex optimization problem. To see this, we calculate the Hessian matrix of the constraint function $-[P_2 g_2(P_3 g_3 + N_0) - P_4 g_4(P_1 g_2 + N_0)]$ as

$$H_{14} = \begin{bmatrix} 0 & 0 & 0 & g_2 g_4 \\ 0 & 0 & -g_2 g_3 & 0 \\ 0 & -g_2 g_3 & 0 & 0 \\ g_2 g_4 & 0 & 0 & 0 \end{bmatrix}. \tag{83}$$

If (14) is a convex function, (83) should be a positive semidefinite matrix. Obviously, this is not the case because not all principal minors of (83) are larger than or equal to 0. Therefore, the constrained minimization problem in (17) is not convex.

APPENDIX B

We discuss the feasibility of the KKT condition for the NDR network given in (19) to (38). In the first step, we examine those in (29), (30), (31), (32) and (38). Since P_1, P_2, P_3 and P_4 are positive numbers which ensures data transmission is performed in both the upper and the lower branches, λ_6, λ_7, λ_8 and λ_9 must be zeros undoubtedly. On the other hand, λ_5 in (28) will be nonnegative if the network exploits all possible transmit power P_t to achieve a higher achievable rate. For this case, (37) can be rewritten as $P_1 + P_2 + P_3 + P_4 = P_t$. Consequently, (29), (30), (31) and (32) are inactive conditions.

Though we exclude (29) through (32) in the optimization, determining whether λ_1 and λ_2 are zeros or positive numbers is still hard. To reveal this, we temporarily change to discuss whether C_1 equals C_3 and C_2 equals C_4. In (8) and (9), we see that both $C_1 > C_3$ and $C_2 > C_4$ imply the interior solution of problem, which indicates the inflow of data information is strictly larger than its corresponding outflow. This imbalance unavoidably lets the power resource be wasted in the first transmission phase. Thus, $C_1 = C_3$ and $C_2 = C_4$ are expected for the optimal solution. Such critical conditions are called *flow balance* in this work. Therefore, we can readily conclude that $C_1 = C_3$ and $C_2 = C_4$, and this directly gives

$$P_3 = \frac{g_1}{g_3} P_1 \tag{84}$$

$$P_4 = \frac{g_2}{g_4} \frac{P_3 g_3 + N_0}{P_1 g_2 + N_0} P_2. \tag{85}$$

which also implies λ_1 and λ_2 are just nonnegative numbers. Next, we change our focus to (26) and (27). To be more specific, λ_3 and λ_4 are nonnegative numbers such that

we can list four cases depending on whether they are zero or nonzero, discuss these cases step by step, and find out whether contradictions exist.

- *Case 1:* $\lambda_3 = 0$ and $\lambda_4 = 0$.
  We need to check if inconsistency occurs among (20), (21), (22), and (23). For this case, we rearrange the terms in (20) to obtain $g_1\lambda_1 = P_4g_2g_4\lambda_2 + \lambda_5$. Since both the left-hand side and the right-hand side are nonnegative numbers, it is valid. Likewise, no contradiction takes place in (21), (22) and (23). Hence, both SIC constraints are adequate and this case holds.

- *Case 2:* $\lambda_3 = 0$ and $\lambda_4 > 0$.
  As $\lambda_4 > 0$, this implies

$$P_4 = \gamma_{\text{th}}\frac{g_3}{g_4}P_3. \tag{86}$$

  We substitute (84) and (86) for P_3 and P_4, respectively, in (85). Then, we have

$$\frac{P_2}{P_1} = \left(\frac{P_1g_1g_2 + N_0g_1}{P_1g_1g_2 + N_0g_2}\right)\gamma_{\text{th}}. \tag{87}$$

  Because we assume $g_1 > g_2$ in the network, $(P_1g_1g_2 + N_0g_1)/(P_1g_1g_2 + N_0g_2)$ should be greater than 1. We can easily conclude that $(P_2/P_1) \geq \gamma_{\text{th}}$ is always true, which also indicates the SIC at R_1 holds.

- *Case 3:* $\lambda_3 > 0$ and $\lambda_4 = 0$.
  When $\lambda_3 > 0$, we have

$$P_2 = \gamma_{\text{th}}P_1. \tag{88}$$

  Similarly, we use (84) and (88) to replace P_3 and P_2, respectively, in (85), and obtain

$$\frac{P_4g_4}{P_3g_3} = \left(\frac{P_1g_1g_2 + N_0g_2}{P_1g_1g_2 + N_0g_1}\right)\gamma_{\text{th}}. \tag{89}$$

  However, $(P_1g_1g_2 + N_0g_2)/(P_1g_1g_2 + N_0g_1)$ is less than 1 due to $g_1 > g_2$, which leads to $\frac{P_4g_4}{P_3g_3} \leq \gamma_{\text{th}}$. This makes the SIC at the destination cannot be accomplished, and the assumption for this case is thus not suitable for the solution.

- *Case 4:* $\lambda_3 > 0$ and $\lambda_4 > 0$.
  It can be inferred that both (86) and (88) hold when $\lambda_3 > 0$ and $\lambda_4 > 0$. Likewise, we substitute these two equations for P_4 and P_2 in (85), and obtain

$$\left(\gamma_{\text{th}}\frac{g_3}{g_4}\right)\left(\frac{g_1}{g_3}P_1\right) = \frac{g_2}{g_4}\left(\frac{P_1g_1 + N_0}{P_1g_2 + N_0}\right)(\gamma_{\text{th}}P_1) \tag{90}$$

  which results in $g_1 = g_2$. This actually contradicts the assumption in the network. Therefore, this case is also not suitable for the solution.

Summarizing the derivations for all these cases, some conditions are simplified, e.g., only Case 1 and Case 2 are valid and $\lambda_6 = \lambda_7 = \lambda_8 = \lambda_9 = 0$, and the solution can be found much easily.

APPENDIX C

From the KKT condition for the C-NDR network listed from (59) to (82). We see that μ_8, μ_9, μ_{10}, μ_{11}, and μ_{12} are zeros because all the power levels should be positive. With the idea of flow balance, we conclude that $C_2 = C_6$ and $C_{34} = C_7$ where μ_3 and μ_4 are just nonnegative numbers. Thus, we obtain

$$P_3 = \frac{g_1}{g_3}P_1 \tag{91}$$

$$\frac{P_2g_2}{P_1g_2 + N_0} + \frac{P_cg_c}{N_0} = \frac{P_4g_4}{P_3g_3 + N_0}. \tag{92}$$

However, we cannot directly assert that $C_1 = C_4$ or $C_1 = C_5$ in the cooperation phase. If these two equations hold simultaneously such that $C_4 = C_5$, the channel gain g_c must be same as g_3. Although this condition rarely happens in practice, we still need to discuss it. All these lead to the following three possibilities: $g_c > g_3$, $g_c < g_3$, and $g_c = g_3$. First, when $g_c > g_3$, the inflow C_1 would mainly contribute to C_4. Thus, we can obtain $C_1 = C_4$ straightforwardly due to the flow-balance concept, and then $\mu_2 = 0$. From the expressions of C_1, C_4 and C_5 given in (41), (44) and (46), respectively, we have

$$\frac{P_2g_1}{P_1g_1 + N_0} = \frac{P_cg_c}{N_0}. \tag{93}$$

Similarly, $C_1 = C_5$ and $\mu_1 = 0$ if $g_c < g_3$. That is,

$$\frac{P_2g_1}{P_1g_1 + N_0} = \frac{P_cg_3}{N_0}. \tag{94}$$

Otherwise, $C_1 = C_4 = C_5$ if $g_c = g_3$, which implies

$$\frac{P_2g_1}{P_1g_1 + N_0} = \frac{P_cg_c}{N_0} = \frac{P_cg_3}{N_0}. \tag{95}$$

In addition, inspecting μ_5 in (69) and μ_6 in (70) derived from the two SIC constraints, we find that

$$P_2 = \gamma_{\text{th}}P_1, \quad \text{if } \mu_5 > 0 \tag{96}$$

$$P_4 = \gamma_{\text{th}}\frac{g_3}{g_4}P_3, \quad \text{if } \mu_6 > 0 \tag{97}$$

which also signifies the use of the SIC constraints. Accordingly, based on the possibilities regarding not only the values of g_c and g_3, but also whether the SIC constraints can be accomplished, we have the following discussion.

1) $g_c > g_3$

- *Case A:* $\mu_5 = 0$ and $\mu_6 = 0$.
  For this case, we need to find out whether there are contradictions among (60), (61), (62), (63) and (64). Take (60) as an example. Since $\mu_2 = \mu_5 = \mu_6 = 0$, we obtain $g_1\mu_3 + g_2g_cP_c(P_3g_3 + N_0)\mu_4 = g_1g_cP_c\mu_1 + N_0g_2g_4P_4\mu_4 + \mu_7$. Both the left-hand side and the right-hand side are nonnegative numbers, and so this result does not contradict our assumption. Likewise, (61), (62), (63), and (64) have no contradiction too.

- *Case B:* $\mu_5 = 0$ and $\mu_6 > 0$.

While $\mu_6 > 0$, it directly implies (97) holds, and so we may substitute (97), (91) and (93) for those in (92), respectively. After some simplification, we obtain

$$\frac{P_2}{P_1} = \left[\frac{P_1 g_1 g_2 + g_1 N_0}{2P_1 g_1 g_2 + (g_1 + g_2)N_0}\right]\gamma_{\text{th}}. \quad (98)$$

It is intuitive that $\dfrac{P_1 g_1 g_2 + g_1 N_0}{2P_1 g_1 g_2 + (g_1 + g_2)N_0}$ is less than 1, which indicates the SIC at R_1 cannot perform successfully due to $(P_2/P_1) < \gamma_{\text{th}}$. Therefore, the assumption here is not appropriate to the solution.

- *Case C:* $\mu_5 > 0$ and $\mu_6 = 0$.
  As $\mu_5 > 0$, (96) holds and we replace those in (92) with (96), (91) and (93). Hence, we have

$$\frac{P_4 g_4}{P_3 g_3} = \left[\frac{2P_1 g_1 g_2 + (g_1 + g_2)N_0}{P_1 g_1 g_2 + g_1 N_0}\right]\gamma_{\text{th}}. \quad (99)$$

It is opposite to Case B where the numerator is greater than the denominator, and this result points out that the SIC at the destination can well perform. Consequently, this assumption is suitable for the solution.

- *Case D:* $\mu_5 > 0$ and $\mu_6 > 0$.
  For this case, (97) and (96) undoubtedly hold at the same time. We replace those in (92) with (91) and (93), and find out that

$$\frac{\gamma_{\text{th}} P_1 g_2}{P_1 g_2 + N_0} = 0. \quad (100)$$

However, all the terms in the nominator in the above expression are nonzero numbers so that it contradicts the assumption in the network model. Therefore, this is not a feasible case.

After that, we summarize these four cases: μ_6 is always zero such that (70) is inactive; however, μ_5 is just a nonnegative number, and (69) is either active or inactive depending on the value of μ_5.

2) $g_c < g_3$

- *Case A:* $\mu_5 = 0$ and $\mu_6 = 0$.
  Here, we apply the same analysis technique used in 1). Because $\mu_1 = \mu_5 = \mu_6 = 0$, (60) can be simplified as $g_1\mu_3 + g_2 g_c P_c(P_3 g_3 + N_0)\mu_4 = g_1 g_3 P_c\mu_2 + \mu_7$. It can be seen that both the left-hand side and the right-hand side are nonnegative numbers, and this result does not contradict our assumption. Similarly, (61), (62), (63) and (64) have no contradiction too.
- *Case B:* $\mu_5 = 0$ and $\mu_6 > 0$.
  When $\mu_6 > 0$, (97) holds, and so we substitute (97), (91), and (94) for those in (92). Afterwards, we obtain

$$\frac{P_2}{P_1} = \left[\frac{P_1 g_1 g_2 g_3 + g_1 g_3 N_0}{P_1 g_1 g_2(g_3 + g_c) + N_0(g_2 g_3 + g_1 g_c)}\right]\gamma_{\text{th}}. \quad (101)$$

Note that it is not straightforward enough to determine either the denominator or the numerator is greater than

the other. However, when $g_c \approx g_3$, we can make an approximation for (101) as

$$\frac{P_2}{P_1} \approx \left[\frac{P_1 g_1 g_2 + g_1 N_0}{2P_1 g_1 g_2 + (g_1 + g_2)N_0}\right]\gamma_{\text{th}}. \quad (102)$$

Since the denominator is larger than the numerator, $\dfrac{P_2}{P_1}$ is less than 1, and it can be inferred that the SIC at R_1 cannot be performed such that Case B does not hold if $g_c \approx g_3$.

- *Case C:* $\mu_5 > 0$ and $\mu_6 = 0$.
  As $\mu_5 > 0$, (96) holds and we replace those in (92) with (96), (91) and (94), and obtain

$$\frac{P_4 g_4}{P_3 g_3} = \left[\frac{P_1 g_1 g_2(g_3 + g_c) + N_0(g_2 g_3 + g_1 g_c)}{P_1 g_1 g_2 g_3 + g_1 g_3 N_0}\right]\gamma_{\text{th}}. \quad (103)$$

We see that the format of (103) is similar to (101), which cannot be easily concluded whether the numerator is greater than the denominator or not. Likewise, if $g_c \approx g_3$, we may have

$$\frac{P_4 g_4}{P_3 g_3} \approx \left[\frac{2P_1 g_1 g_2 + (g_1 + g_2)N_0}{P_1 g_1 g_2 + g_1 N_0}\right]\gamma_{\text{th}}. \quad (104)$$

This special condition ensures that the SIC at the destination can be performed successfully.

- *Case D:* $\mu_5 > 0$ and $\mu_6 > 0$.
  For this case, (97) and (96) hold simultaneously. We replace those in (92) with (91) and (94). It can be seen that

$$P_1 g_1 g_c(P_1 g_2 + N_0) = 0. \quad (105)$$

However, all the terms in the above expression are nonzero nonnegative numbers such that it makes a contradiction, and so this case is not a candidate to the solution.

Although we cannot reduce the KKT condition to some simpler forms due to the diversity of μ_5 and μ_6 in Case B and Case C, we still arrive at a special condition, $g_c \approx g_3$, to let the system operate smoothly. For this special case with $\mu_5 \geq 0$ and $\mu_6 = 0$, the KKT condition can be reduced to become a much simpler system of equations which is the same as that in 1). Additionally, this system of equations can be numerically solved by MATLAB, and the boundary conditions of each variable in the solution set can be checked accordingly.

3) $g_c = g_3$

In this part, as stated, the assumption $g_c = g_3$ gives $C_1 = C_4 = C_5$ while the other conditions are the same as those in 1). Hence, all derivations in 1) are still valid here, and so we need not discuss them again.

APPENDIX D

As said, the SOSC is employed to check if the critical points found by KKT theorem are the strict local minimizers we expect. For easy understanding, partly based on the settings in Table 1, we typically set $g_1 = 10$, $g_2 = 3$, $g_3 = 5$, $g_4 = 9$, $\gamma_{th} = 5$, $P_t = 2$, and $N_0 = 10^{-2}$ in the calculation. By the KKT condition, we find that $P_1 = 0.04784$, $P_2 = 0.9010$, $P_3 = 0.09568$, $P_4 = 0.9555$, $\lambda_1 = 0.9484$, $\lambda_2 = 0.3479$, $\lambda_5 = 0.5097$ and $\lambda_3 = \lambda_4 = \lambda_6 = \lambda_7 = \lambda_8 = \lambda_9 = 0$. Then, we need to find the Hessian of (18) for use in the SOSC. Based on the results in (20)-(23), performing differentiation yields the Hessian $\mathbf{H}_L$ as

$$\mathbf{H}_L = \begin{bmatrix} H_{11} & \cdots & H_{14} \\ \vdots & \ddots & \vdots \\ H_{41} & \cdots & H_{44} \end{bmatrix} \tag{106}$$

in which $H_{11} = H_{12} = H_{13} = H_{21} = H_{22} = H_{24} = H_{31} = H_{42} = 0$ and

$$H_{14} = H_{41} = g_2 g_4 \lambda_2 \tag{107}$$

$$H_{23} = H_{32} = -g_2 g_3 \lambda_2 \tag{108}$$

$$H_{33} = \frac{P_4^2 g_3^2 g_4^2}{(1+\gamma_4)^2 (1+\gamma_3)^4 N_0^4} + \frac{g_3^2}{(1+\gamma_3)^2 N_0^2}$$
$$- \frac{2 P_4 g_3^2 g_4}{(1+\gamma_4)(1+\gamma_3)^3 N_0^3} \tag{109}$$

$$H_{34} = H_{43}$$
$$= \frac{g_3 g_4}{(1+\gamma_4)(1+\gamma_3)^2 N_0^2} - \frac{P_4 g_3 g_4^2}{(1+\gamma_4)^2 (1+\gamma_3)^3 N_0^3} \tag{110}$$

$$H_{44} = \frac{g_4^2}{(1+\gamma_4)^2 (1+\gamma_3)^2 N_0^2} \tag{111}$$

with the notations $\gamma_3 = \frac{P_3 g_3}{N_0}$ and $\gamma_4 = \frac{P_4 g_4}{P_3 g_3 + N_0}$. Substituting the power levels found by the KKT condition and the parameters used here into (106), we obtain

$$\mathbf{H}_L = \begin{bmatrix} 0 & 0 & 0 & 9.3923 \\ 0 & 0 & -5.2179 & 0 \\ 0 & -5.2179 & 0.3027 & 0.5449 \\ 9.3923 & 0 & 0.5449 & 0.9808 \end{bmatrix}. \tag{112}$$

According to the SOSC, we compute the differentiation of the active constraints according to the nonzero λ_1, λ_2 and λ_5 as

$$\nabla f_1 = \begin{bmatrix} -g_1 & 0 & g_3 & 0 \end{bmatrix}^T$$
$$= +[-10 \ 0 \ 5 \ 0]^T \tag{113}$$

$$\nabla f_2 = \begin{bmatrix} P_4 g_2 g_4 & -g_2(P_3 g_3 + N_0) \\ & -P_2 g_2 g_3 & g_4(P_1 g_2 + N_0) \end{bmatrix}^T$$
$$= [25.7977 \ -1.4652 \ -13.5151 \ 1.3817]^T \tag{114}$$

$$\nabla f_5 = [1 \ 1 \ 1 \ 1]^T \tag{115}$$

where f_1, f_2 and f_5 denote the first, the second, and the fifth constraints in (17), respectively. Based on these gradient vectors, we may numerically find the nonzero vector

$\mathbf{x}$ satisfying $[\nabla f_1 \ \nabla f_2 \ \nabla f_5]^T \mathbf{x} = \mathbf{0}$. As a result, the most important part in the SOSC, i.e., $\mathbf{x}^T \mathbf{H}_L \mathbf{x}$, can be calculated and shown to be larger than zero. This positive value lets the solution found by KKT theorem be the strict local minimizer for this case. Likewise, all the power levels found by the KKT condition undergo this kind of checking to guarantee that they are effective to maximize the overall achievable rate of the network.

REFERENCES

[1] Y. Saito, Y. Kishiyama, A. Benjebbour, T. Nakamura, A. Li, and K. Higuchi, "Non-orthogonal multiple access (NOMA) for cellular future radio access," in *Proc. 77th VTC Spring*, Dresden, Germany, Jan. 2013, pp. 1–5.

[2] L. Dai, B. Wang, Y. Yuan, S. Han, C.-L. I, and Z. Wang, "Non-orthogonal multiple access for 5G: Solutions, challenges, opportunities, and future research trends," *IEEE Commun. Mag.*, vol. 53, no. 9, pp. 74–81, Sep. 2015.

[3] S. M. R. Islam, N. Avazov, O. A. Dobre, and K.-S. Kwak, "Power-domain non-orthogonal multiple access (NOMA) in 5G systems: Potentials and challenges," *IEEE Commun. Surveys Tuts.*, vol. 19, no. 2, pp. 721–742, 2nd Quart., 2017.

[4] A. Nosratinia, T. E. Hunter, and A. Hedayat, "Cooperative communication in wireless networks," *IEEE Commun. Mag.*, vol. 42, no. 10, pp. 74–80, Oct. 2004.

[5] B. Wang, J. Zhang, and A. Host-Madsen, "On the capacity of MIMO relay channels," *IEEE Trans. Inf. Theory*, vol. 51, no. 1, pp. 29–43, Jan. 2005.

[6] K. Loa *et al.*, "IMT-advanced relay standards," *IEEE Commun. Mag.*, vol. 48, no. 8, pp. 40–48, Aug. 2010.

[7] C. Hoymann, W. Chen, J. Montojo, A. Golitschek, C. Koutsimanis, and X. Shen, "Relaying operation in 3GPP LTE: Challenges and solution," *IEEE Commun. Mag.*, vol. 50, no. 2, pp. 156–162, Feb. 2012.

[8] R.-A. Pitaval, O. Tirkkonen, R. Wichman, K. Pajukoski, E. Lahetkangas, and E. Tiirola, "Full-duplex self-backhauling for small-cell 5G networks," *IEEE Wireless Commun.*, vol. 22, no. 5, pp. 83–89, Oct. 2015.

[9] Z. Chen, T. Li, P. Fan, T. Q. S. Quek, and K. B. Letaief, "Cooperation in 5G heterogeneous networking: Relay scheme combination and resource allocation," *IEEE Trans. Commun.*, vol. 64, no. 8, pp. 3430–3443, Aug. 2016.

[10] J. Deng, O. Tirkkonen, R. Freij-Hollanti, T. Chen, and N. Nikaein, "Resource allocation and interference management for opportunistic relaying in integrated mmWave/sub-6 5G networks," *IEEE Commun. Mag.*, vol. 55, no. 6, pp. 94–101, Jun. 2017.

[11] Y. Hu, M. C. Gursoy, and A. Schmeink, "Relaying-enabled ultra-reliable low-latency communications in 5G," *IEEE Netw.*, vol. 32, no. 2, pp. 62–68, Mar./Apr. 2018.

[12] Z. Ding, M. Peng, and H. V. Poor, "Cooperative non-orthogonal multiple access in 5G systems," *IEEE Commun. Lett.*, vol. 19, no. 8, pp. 1462–1465, Aug. 2015.

[13] J.-B. Kim and I.-H. Lee, "Capacity analysis of cooperative relaying systems using non-orthogonal multiple access," *IEEE Commun. Lett.*, vol. 19, no. 11, pp. 1949–1952, Nov. 2015.

[14] D. Wan, M. Wen, J. Ji, H. Yu, and F. Chen, "Non-orthogonal multiple access for cooperative communications: Challenges, opportunities, and trends," *IEEE Wireless Commun.*, vol. 25, no. 2, pp. 107–117, Apr. 2018.

[15] Z. Ding, H. Dai, and H. V. Poor, "Relay selection for cooperative NOMA," *IEEE Wireless Commun. Lett.*, vol. 5, no. 4, pp. 416–419, Aug. 2016.

[16] Z. Yang, Z. Ding, Y. Wu, and P. Fan, "Novel relay selection strategies for cooperative NOMA," *IEEE Trans. Veh. Technol.*, vol. 66, no. 11, pp. 10114–10123, Nov. 2017.

[17] P. Xu, Z. Yang, Z. Ding, and Z. Zhang, "Optimal relay selection schemes for cooperative NOMA," *IEEE Trans. Veh. Technol.*, vol. 67, no. 8, pp. 7851–7855, Aug. 2018.

[18] Z. Yu, C. Zhai, J. Liu, and H. Xu, "Cooperative relaying based non-orthogonal multiple access (NOMA) with relay selection," *IEEE Trans. Veh. Technol.*, vol. 67, no. 12, pp. 11606–11618, Dec. 2018.

[19] R.-H. Gau, H.-T. Chiu, C.-H. Liao, and C.-L. Wu, "Optimal power control for NOMA wireless networks with relays," *IEEE Wireless Commun. Lett.*, vol. 7, no. 1, pp. 22–25, Feb. 2018.

[20] S. Wang, S. Cao, and R. Ruby, "Optimal power allocation in NOMA-based two-path successive AF relay systems," *EURASIP J. Wireless Commun. Netw.*, vol. 2018, p. 273, Dec. 2018.

[21] Q. Wang and F. Zhao, "Joint spectrum and power allocation for NOMA enhanced relaying networks," *IEEE Access*, vol. 7, pp. 27008–27016, 2019.

[22] W. Duan, J. Ju, J. Hou, Q. Sun, X.-Q. Jiang, and G. Zhang, "Effective resource utilization schemes for decode-and-forward relay networks," *IEEE Access*, vol. 7, pp. 51466–51474, 2019.

[23] O. Abbasi, A. Ebrahimi, and N. Mokari, "NOMA inspired cooperative relaying system using an AF relay," *IEEE Wireless Commun. Lett.*, vol. 8, no. 1, pp. 261–264, Feb. 2019.

[24] X. Liang, Y. Wu, D. W. K. Ng, Y. Zuo, S. Jin, and H. Zhu, "Outage performance for cooperative NOMA transmission with AF relay," *IEEE Commun. Lett.*, vol. 21, no. 11, pp. 2428–2431, Nov. 2017.

[25] Y. Xiao, L. Hao, Z. Ma, Z. Ding, Z. Zhang, and P. Fan, "Forwarding strategy selection in dual-hop NOMA relaying systems," *IEEE Commun. Lett.*, vol. 22, no. 8, pp. 1644–1647, Aug. 2018.

[26] H. Liu, Z. Ding, K. J. Kim, K. S. Kwak, and H. V. Poor, "Decode-and-forward relaying for cooperative NOMA systems with direct links," *IEEE Trans. Wireless Commun.*, vol. 17, no. 12, pp. 8077–8093, Dec. 2018.

[27] L. Zhang, J. Liu, M. Xiao, G. Wu, Y.-C. Liang, and S. Li, "Performance analysis and optimization in downlink NOMA systems with cooperative full-duplex relaying," *IEEE J. Sel. Areas Commun.*, vol. 35, no. 10, pp. 2398–2412, Oct. 2017.

[28] X. Yue, Y. Liu, S. Kang, A. Nallanathan, and Z. Ding, "Exploiting full/half-duplex user relaying in NOMA systems," *IEEE Trans. Commun.*, vol. 66, no. 2, pp. 560–575, Feb. 2018.

[29] X. Yue, Y. Liu, S. Kang, A. Nallanathan, and Z. Ding, "Spatially random relay selection for full/half-duplex cooperative NOMA networks," *IEEE Trans. Commun.*, vol. 66, no. 8, pp. 3294–3308, Aug. 2018.

[30] Z. Wang, X. Yue, and Z. Peng, "Full-duplex user relaying for NOMA system with self-energy recycling," *IEEE Access*, vol. 6, pp. 67057–67069, 2018.

[31] L. Bariah, S. Muhaidat, and A. Al-Dweik, "Error probability analysis of NOMA-based relay networks with SWIPT," *IEEE Commun. Lett.*, vol. 22, no. 8, pp. 1644–1647, Jul. 2019.

[32] H. Q. Tran, T.-T. Nguyen, C. V. Phan, and Q.-T. Vien, "Power-splitting relaying protocol for wireless energy harvesting and information processing in NOMA systems," *IET Commun.*, vol. 13, no. 14, pp. 2132–2140, 2019.

[33] N. T. Do, D. B. Da Costa, T. Q. Duong, and B. An, "A BNBF user selection scheme for NOMA-based cooperative relaying systems with SWIPT," *IEEE Commun. Lett.*, vol. 21, no. 3, pp. 664–667, Mar. 2017.

[34] D. Wan, M. Wen, H. Yu, Y. Liu, F. Ji, and F. Chen, "Non-orthogonal multiple access for dual-hop decode-and-forward relaying," in *Proc. IEEE Global Commun. Conf.*, Washington, DC, USA, Dec. 2016, pp. 1–6.

[35] D. Wan, M. Wen, F. Ji, H. Yu, and F. Chen, "On the achievable sum-rate of NOMA-based diamond relay networks," *IEEE Trans Veh. Technol.*, vol. 68, no. 2, pp. 1472–1486, Feb. 2019.

[36] E. K. P. Chong and S. H. Zak, *An Introduction to Optimization*, 4th ed. New York, NY, USA: Wiley, 2013.

[37] F. Fang, Z. Ding, W. Liang, and H. Zhang, "Optimal energy efficient power allocation with user fairness for uplink MC-NOMA systems," *IEEE Wireless Commun. Lett.*, vol. 8, no. 4, pp. 1133–1136, Aug. 2019.

BO-YING HUANG received the B.S. degree from the Department of Electrical Engineering, National Cheng Kung University (NCKU), Tainan, Taiwan, in 2017, and the M.S. degree from the Institute of Computer and Communication Engineering, NCKU, in 2019. He is currently in military service. His current research interests include full-duplex networks, nonorthogonal multiple access, and wireless communications.

YINMAN LEE (Member, IEEE) received the Ph.D. degree from the Department of Communication Engineering, National Chiao Tung University, Hsinchu, Taiwan, in 2006. He is currently a Professor with the Department of Electrical Engineering, National Chi Nan University, Puli, Taiwan. His research interests include system optimization, adaptive signal processing, wireless communications, and multiple antenna systems.

SOK-IAN SOU (Member, IEEE) received the B.S., M.S., and Ph.D. degrees in computer science and information engineering from National Chiao Tung University, Hsinchu, Taiwan, in 1997, 2004, and 2008, respectively. She is a Professor with the Institute of Computer and Communication Engineering and the Department of Electrical Engineering, National Cheng Kung University, Tainan, Taiwan. She was a Visiting Scholar with Carnegie Mellon University from July 2009 to August 2009. She has coauthored the book titled *Charging for Mobile All-IP Telecommunications* (with Yi-Bing Lin; Wiley, 2008). Her current research interests include Internet of Things, mobile networks, and wireless sensing. She was a recipient of the Investigative Research Award from the Pan Wen Yuan Foundation in 2009, the Young Researcher in Service Science Award from the Sayling Wen Cultural and Educational Foundation in 2012, and the Outstanding Teacher Award in 2017.